Measurements of the Rise Velocities of Bubbles, Slugs and Pressure Waves in a Gas-Solid Fluidized Bed Using Pressure Fluctuation Signals

The rise velocities of bubbles, slugs and pressure waves in a fluidized bed have been measured on-line through the use of pressure transducers coupled with the cross-correlation technique. Sand and glass beads with different particle sizes were tested. Effects of the gas flow rate and column diameter on the rise velocities of bubbles and slugs were investigated. The results were correlated with two models developed in this work and were compared with the data obtained by other investigators.

L. T. FAN, THO-CHING HO and W. P. WALAWENDER

Department of Chemical Engineering
Kansas State University
Manhattan, KS 66506

SCOPE

In a gas-solid fluidized bed, bubbles form near the distributor, coalesce, grow, and increase in velocity as they rise through the bed. Knowledge of the rise velocity of gas bubbles is important, since it is one of the factors determining the gas residence time in the bed. It has been observed that the rise velocity of bubbles is directly related to the bubble size, which governs the quality of fluidization and the rate of mass or heat transfer between the dilute and dense phases.

The rise velocity of an isolated spherical capped bubble has been determined to approximately obey the expression

$$U_b = k(gD_b)^{1/2} \tag{1}$$

where k varies between 0.57 and 0.85 (Davidson et al., 1959; Harrison and Leung, 1961; Reuter, 1963; Rowe and Partridge, 1965; Kunii and Levenspiel, 1969). When the diameter of the bubble becomes comparable to that of the containing vessel, the rise velocity becomes independent of its volume and is given by (Ormiston et al., 1965)

$$U_s = 0.35(gD_t)^{1/2} \tag{2}$$

In bubbling beds, a bubble rises in the company of a crowd of rising bubbles, and the absolute rise velocity of the bubble is given by Davidson and Harrison (1963) as

$$\begin{aligned} V_b &= (U - U_{mf}) + U_b \\ &= (U - U_{mf}) + k(gD_b)^{1/2} \end{aligned} \tag{3}$$

For slugging beds, the velocity of the gas slug has been measured by Davidson and Harrison (1963), Ormiston et al. (1965), and Matsen et al. (1969) as

$$\begin{aligned} V_s &= k'(U - U_{mf}) + U_s \\ &= k'(U - U_{mf}) + 0.35\,(gD_t)^{1/2} \end{aligned} \tag{4}$$

where k' ranges between 0.87 and 9.68.

Various experimental techniques for measuring the bubble rise velocity were used in the previous studies. The techniques included: photographing with ordinary cameras (Pyle and Harrison, 1967a, 1967b; Godard and Richardson, 1969) or with X-ray cameras (Rowe and Partridge, 1965; Toei et al., 1965); and sensing with capacitance probes (Lanneau, 1960; Toei et al., 1965; Ormiston et al., 1965; Werther and Molerus, 1973) or electroresistivity probes (Park et al., 1969; Rigby et al., 1970). The pressure transducer technique was also employed in measuring the rise velocity of bubbles in a fluidized bed. Littman and Homolka (1970) determined bubble rise velocities in a two-dimensional fluidized bed from pressure-time curves detected by a pressure transducer. Swinehart (1966) determined bubble rise velocities in a fluidized bed by calculating off-line the cross-correlation function between two pressure fluctuation signals, which were taken simultaneously from two vertically separated pressure taps. While the correlation technique has been demonstrated to be a powerful tool in determining the bubble rise velocity, the excessive time and effort needed to employ it for off-line calculation have prevented its widespread use.

In this work, a totally on-line approach was used to cross-correlate pressure fluctuation signals for determining the rise velocities of bubbles, slugs and pressure waves in a three-dimensional gas-solid fluidized bed. Pressure transducers were used to detect the pressure fluctuations and a correlation and probability analyzer was used for on-line calculation of the cross-correlation functions. Sand and glass beads with different particle sizes were tested. Effects of the fluidizing gas flow rate and column diameter on the rise velocities of bubbles and slugs were investigated. The results were correlated with two models developed in this work and were compared with the data obtained by other investigators.

CONCLUSIONS AND SIGNIFICANCE

It has been demonstrated that the rise velocities of bubbles, slugs, or pressure waves in a fluidized bed can be measured on-line through the use of pressure transducers coupled with the cross-correlation technique. The measured results were compared with the data observed by other investigators, and good agreement was obtained. The two models proposed appear to describe the experimental data reasonably well.

For a fluidized bed with a relatively large column diameter

0001-1541-83-6468-0033-$2.00

(e.g., $D_t \geq 0.2$ m), the experimental results show that, as the gas flow rate exceeds the minimum fluidization velocity, three operating regimes, bubbling, slugging and turbulent, will appear in succession in the bed with the increase in the gas flow rate. However, the turbulent bed regime is not observed in a fluidized bed with a relatively small column diameter.

While most of the previous studies employed visual observation to determine the onset of slugging, the present technique enables us to determine it on-line and instrumentally using the rise velocity of the bubbles or slugs as the criterion. Because the rise velocities and the operating regime in the bed are determined on-line, potential applications of the present technique in process design and control of pilot plants or production facilities are obvious.

THEORETICAL

The cross-correlation function between two continuous, stationary and ergodic random variables, $X(t)$ and $Y(t)$, is expressed as

$$\phi_{xy}(\tau) = \lim_{T\to\infty} \frac{1}{T} \int_{-T/2}^{T/2} x(t)y(t+\tau)dt \tag{5}$$

where $x(t)$ is the value of $X(t)$ sampled at time (t), and $y(t+\tau)$ is the value of $Y(t)$ sampled at time $(t+\tau)$ (e.g., Lee, 1960). In this work, $X(t)$ and $Y(t)$ are, respectively, pressure fluctuation signals detected at a location upstream and another location downstream. The average time required for a fluctuation waveform to travel between these two locations is the transit time, τ_m, where the cross-correlation function is maximum (Swinehart, 1966; Werther and Molerus, 1973; Oki et al., 1977; Oki et al., 1978). The velocity of the fluctuation waveform, V_f, can be calculated as

$$V_f = \frac{L}{\tau_m} \tag{6}$$

where L is the known distance between the two detecting locations.

It has been pointed out (Swinehart, 1966; Kang et al., 1967; Fan et al., 1981) that the motion of bubbles causes the pressure fluctuations in the upper portion of a fluidized bed. In the case where only a single bubble is observed to pass a horizontal plane at a time, each periodic waveform in the detected pressure-time curve obviously corresponds to the passing of one single bubble. The velocity of a fluctuation waveform, V_f, defined by Eq. 6, is essentially the average rise velocity of bubbles, slugs or pressure waves, respectively, in each bed regime, i.e.,

$$\left.\begin{aligned} V_f &= V_b \text{ (in the bubbling bed regime)} \\ V_f &= V_s \text{ (in the slugging bed regime)} \\ V_f &= V_t \text{ (in the turbulent bed regime)} \end{aligned}\right\} \tag{7}$$

Two models, Model I and Model II, are presented in this work to describe the rise velocities of bubbles, slugs and pressure waves in a fluidized bed.

Model I is based on postulations that the rise velocity of an isolated bubble or an isolated slug is, respectively, a function of the bubble diameter or the bed diameter only, and that the rise of bubbles or slugs is promoted by an upward movement of the dense phase (Davidson and Harrison, 1963). Thus, the rise velocity of bubbles, V_b, can be related to the velocity of the upward movement of the dense phase, $U - U_{mf}$, and the bubble diameter, D_b, as

$$V_b = k_1(U - U_{mf}) + k_2(gD_b)^{1/2} \tag{8}$$

and similarly the rise velocity of slugs, V_s, can be related to the term, $U - U_{mf}$, and the bed diameter, D_t, as

$$V_s = k_1'(U - U_{mf}) + k_2'(gD_t)^{1/2} \tag{9}$$

These two expressions for the bubbling bed regime and the slugging bed regime are essentially identical to Eqs. 3 and 4 except that two parameters are used instead of one. Furthermore, based on the experimental observations, which will be delineated later, Model I postulates that the upward moving velocity of pressure waves in the turbulent bed regime is essentially constant, i.e.,

$$V_t \simeq V_{ta} = \text{constant} \tag{10}$$

Model II is more empirical in nature than Model I. In the former, the dimensionless or normalized rise velocity of bubbles, slugs or pressure waves, defined as

$$\left[\frac{V_b - V_{bmi}}{V_{bma} - V_{bmi}}\right], \left[\frac{V_s - V_{smi}}{V_{sma} - V_{smi}}\right] \quad \text{or} \quad \left(\frac{V_t}{V_{ta}}\right),$$

respectively, are assumed to be power functions of the dimensionless or normalized fluidization gas flow rate, defined as

$$\left[\frac{U - U_{mf}}{U_{ms} - U_{mf}}\right], \left[\frac{U - U_{ms}}{U_{mt} - U_{ms}}\right] \quad \text{or} \quad \left[\frac{U - U_{mt}}{U_t - U_{mt}}\right],$$

respectively, in each bed regime. The behavior of bubbles in the bubbling bed regime is profoundly affected by the bed properties, e.g., the particle size and the particle density; therefore, the exponent of the postulated power function in this bed regime is considered to be a function of the dimensionless particle size and the dimensionless particle density, i.e.,

$$\left.\begin{aligned} \left[\frac{V_b - V_{bmi}}{V_{bma} - V_{bmi}}\right] &= \left[\frac{U - U_{mf}}{U_{ms} - U_{mf}}\right]^{\alpha(\overline{D}_p/D_t)^{\beta}(\rho_s/\rho_f)^{\gamma}} \\ \text{or} \\ ln\left[\frac{V_b - V_{bmi}}{V_{bma} - V_{bmi}}\right] &= \alpha\left(\frac{\overline{D}_p}{D_t}\right)^{\beta}\left(\frac{\rho_s}{\rho_f}\right)^{\gamma} ln\left[\frac{U - U_{mf}}{U_{ms} - U_{mf}}\right] \end{aligned}\right\} \tag{11}$$

The behavior of slugs in the slugging bed regime is assumed to be influenced mostly by the characteristics of the column wall and is affected only slightly by the particle properties and the column size; thus, the exponent of the postulated power function in this bed regime is considered to be constant, i.e.,

$$\left.\begin{aligned} \left[\frac{V_s - V_{smi}}{V_{sma} - V_{smi}}\right] &= \left[\frac{U - U_{ms}}{U_{mt} - U_{ms}}\right]^{\alpha'} \\ \text{or} \\ ln\left[\frac{V_s - V_{smi}}{V_{sma} - V_{smi}}\right] &= \alpha' ln\left[\frac{U - U_{ms}}{U_{mt} - U_{ms}}\right] \end{aligned}\right\} \tag{12}$$

As in the case of Model I, the velocity of pressure waves in the turbulent bed regime is assumed to be constant in this model; thus, we can write

$$\left.\begin{aligned} \left(\frac{V_t}{V_{ta}}\right) &= \left[\frac{U - U_{mt}}{U_t - U_{mt}}\right]^0 \\ \text{or} \\ V_t &\simeq V_{ta} = \text{constant} \end{aligned}\right\} \tag{13}$$

EXPERIMENTAL

The facilities and procedure used in carrying out the experiments and measurements are described in this section.

Facilities

A schematic diagram of the experimental equipment is shown in Figure 1. The fluidized bed assembly included a bed column, a gas distributor and a plenum column. The bed and plenum columns, which were fabricated from "plexiglas" to permit visual observation, were 2 m and 0.17 m long, respectively. Columns of three different diameters, i.e., 0.102 m (4 in.), 0.153 m (6 in.) and 0.203 m (8 in.), were tested. The gas distributor was a perforated aluminum plate 0.00159 m ($\frac{1}{16}$ in.) thick and had holes, each

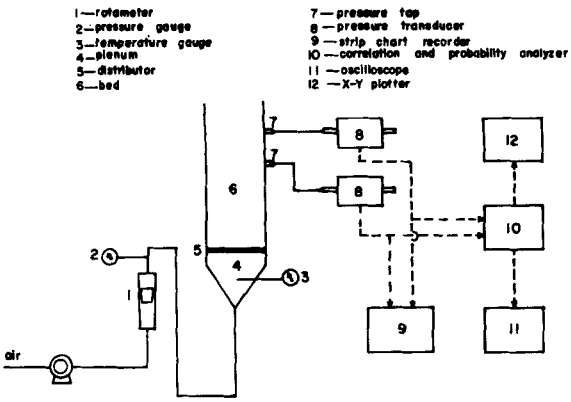

Figure 1. The experimental facilities.

with a diameter of 0.00159 m ($\frac{1}{16}$ in.), drilled in the pattern shown in Figure 2. Five groups of solids were used as the fluidizing particles. Their physical properties are summarized in Table 1. The values of U_{mf} listed were determined experimentally from the pressure drop vs. gas flow rate curve. Air was used as the fluidizing gas for all experiments.

Pressure taps were installed vertically along the columns. The inside opening of each tap was covered with a screen to prevent the sand from entering the tap. The outside opening of a tap was connected to a differential pressure transducer (Enterprise Model CD3J, natural frequency around 5 kHz), which had two input channels and produced an output voltage proportional to the pressure difference between the two input channels. In measuring the pressure fluctuations at a specific location (tap), the tap was connected to the positive input channel while the other channel was left exposed to the atmosphere. With the use of interchangeable diaphragms, the transducers provided a multi-range working capacity. Two transducers, each with a diaphragm capacity of ±20.67 kPa (±3 psi), were used. The lines which connected the taps and the transducers were balanced so that constant transient response could be maintained.

The calculating assembly included a correlation and probability analyzer (Honeywell Model SAI-43A) and an oscilloscope. The analyzer executed calculations of the cross-correlation functions of the fluctuation signals. The recording apparatus included a strip chart recorder and an *X-Y* plotter. The strip chart recorder registered the pressure-time signal from the transducer. It had two input channels so that the pressure-time curves at two locations (taps) could be simultaneously recorded and compared.

Measurements and Calculations

Measurements of the bubble or slug rise velocity were conducted in the upper portion of the bed where only one bubble at a time was observed to pass a horizontal plane. The static bed height at the onset of fluidization for all the experiments was 0.60 m, and the two pressure taps were located at 0.4 m and 0.59 m above the distributor. The range of air flow rate tested was between U_{mf} and the air flow rate where the bed expansion ratio, H/H_{mf}, was approximately equal to 3. For each run with a specific combination of experimental variables, pressure fluctuations at the two pressure taps were detected by connecting the taps to the two pressure transducers. The two voltage-time (corresponding to pressure time) signals, simultaneously taken, were sent to both the strip chart recorder and the correlation and probability analyzer. The recorder registered the pressure-time curves, and the analyzer calculated the cross-correlation function between the two fluctuation signals. The sampling interval for the calculation was selected

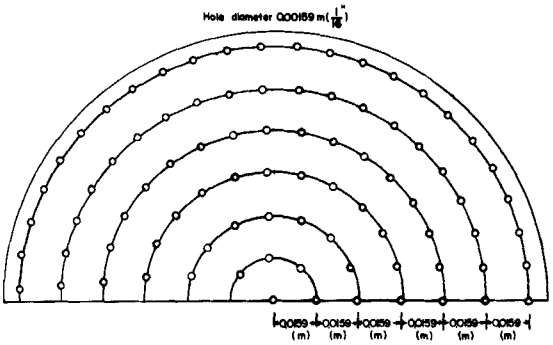

Figure 2. Hole layout of the distributor.

TABLE 1. PHYSICAL PROPERTIES OF FLUIDIZING PARTICLES

Material	U.S. Standard Sieve No.	$\bar{D}_p$(m)	Density (kg/m^3)	U_{mf} (m/s)
sand	14–20	0.001122	2,650	0.66
sand	20–30	0.000711	2,640	0.36
sand	30–40	0.000491	2,620	0.20
Glass Beads	30–40	0.000491	2,430	0.28
Glass Beads	40–50	0.000358	2,400	0.16

to be 1 ms, and a total of 64 × 1,024 points were sampled and calculated. The on-line measurements of the time shift, τ_m, were made on an oscilloscope with the help of a bin marker on the analyzer. The distance between the two taps was known and the average rise velocities of bubbles, slugs, and pressure waves were determined from Eq. 7.

RESULTS AND DISCUSSION

Typical recorded pressure fluctuation signals, calculated cross-correlation functions and calculated rise velocities of bubbles, slugs, or pressure waves are illustrated in the Figures 3 through 6. Typical pressure-time signals are shown in Figure 3. Each pair of pressure fluctuation signals shown in the figure was taken simultaneously from the two pressure taps in the fluidized bed whose operating conditions are cited in the figure. The lower curve of each pair was taken from the tap located at 0.4 m above the distributor and the upper curve was taken from the tap located at 0.59 m above the distributor. The figure indicates that the two curves do not coincide; the upper curve lags behind the lower one. The lag or delay time is considered the traveling time of bubbles or slugs from the lower tap to the upper tap. It can be observed that the delay time is shorter and that the signals are more irregular in shape for the pair of signals with the higher air flow rate than those for the pair with the lower air flow rate.

The cross-correlation functions calculated on-line are shown in Figure 4; they confirm the observation that the delay time between the two pressure fluctuation signals decreases as the air flow rate increases. This appears to be reasonable, since it implies that the rise velocity of bubbles or slugs increases with the air flow rate. The figure also indicates that each of the calculated cross-correlation functions has a relatively flat peak. In calculating the rise velocity, two velocities were first determined based on the value of τ_m at both ends of the flat peak by means of Eq. 6. Their arithmetic average is considered to be the average rise velocity of bubbles or slugs for the measurement.

Figure 5 shows typical results obtained for the bed with a column diameter of 0.203 m (8 in.). It shows that the rise velocity increases with the air flow rate for U/U_{mf} between 1.19 and 1.44. The rise velocity decreases for U/U_{mf} between 1.44 and 1.55, and then increases again until $U/U_{mf} = 2.10$. It fluctuates appreciably when U/U_{mf} is greater than 2.10.

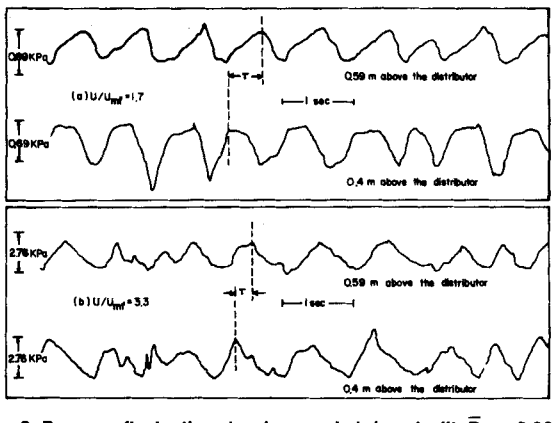

Figure 3. Pressure fluctuation signals recorded. (sand with $\bar{D}_p$ = 0.000711 m, D_t = 0.203 m)

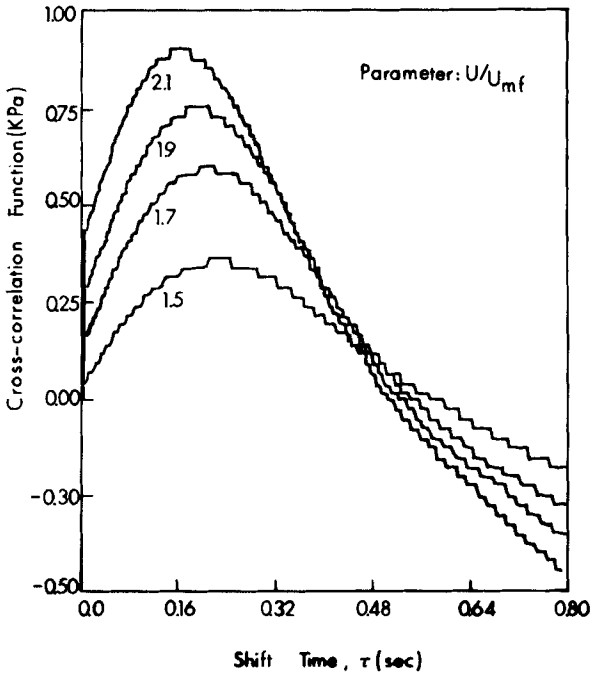

Figure 4. Cross-correlation functions calculated. (sand with $\overline{D}_p$ = 0.000711 m, D_t = 0.203 m)

The decrease in the rise velocity around U/U_{mf} = 1.44 was visually confirmed to be due to the slugging effect, i.e., the diameter of the bubbles became comparable to that of the bed, and the friction between the bed wall and the bubbles became active to reduce the rise velocity of bubbles. The fluctuation in the rise velocity beyond U/U_{mf} = 2.10 was probably caused by the bed turbulence. Visual observation confirmed that the slugging bed was transformed to the turbulent bed at this higher air flow rate, and thus, the velocities fluctuate. It is apparent from the results that, in the 0.203 m diameter column, the bed experienced all three regimes—the bubbling bed, slugging bed and turbulent bed—with the increase in the air flow rate. These three regimes were also observed when other fluidizing particles were tested in this column.

Figure 6 shows typical experimental results for the bed with a column diameter of 0.102 m (4 in.). It clearly indicates the occurrence of the slug effect; however, it exhibits no turbulent effect. This is plausible because there is insufficient space for a rising slug to become turbulent in this smaller column. The results from fluidized beds, each with a column diameter of 0.153 m (6 in.), exhibit all three bed regimes for relatively small fluidizing particles

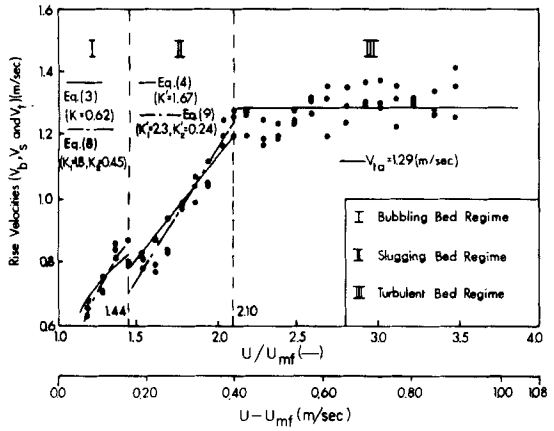

Figure 5. Plot of the rise velocities of bubbles, slugs and pressure waves against the dimensionless air flow rate. (sand with $\overline{D}_p$ = 0.000711 m, D_t = 0.203 m)

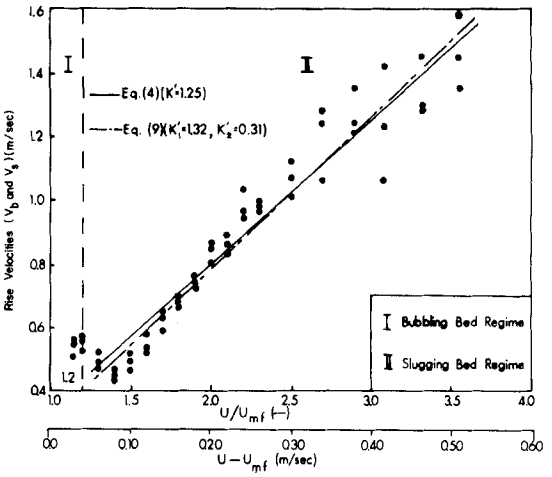

Figure 6. Plot of the rise velocities of bubbles and slugs against the dimensionless air flow rate. (sand with $\overline{D}_p$ = 0.000711 m, D_t = 0.102 m)

(e.g., $\overline{D}_p \leq 0.00035$ m); however, no clear turbulent bed regime was observed for the beds with relatively large fluidizing particles (e.g., $\overline{D}_p \leq 0.00036$ m).

Onset of Slugging

The technique employed in this work enables us to determine the onset of slugging using the rise velocity as the criterion. The onset of slugging in this work is defined to be the air flow rate at which the rise velocity starts to decline in the transition between the bubbling bed and slugging bed regimes, e.g., U/U_{mf} = 1.44 in Figure 5, or U/U_{mf} = 1.2 in Figure 6. The velocities at the onset of slugging observed in this work are compared with the data correlated by Stewart (Davidson and Harrison, 1971) in Figure 7. It can be seen that the agreement is good.

The experimental results were correlated with Model I, Model II and the available models; they are discussed in the following paragraphs.

Model I

Model I as well as the available models (Eqs. 3 and 4) were fitted to the experimentally determined rise velocities of bubbles and slugs. The results are shown in Figures 5 and 6. Notice that, in the bubbling bed regime, the bubble diameter corresponding to each measured rise velocity was estimated using the equation derived by Darton et al. (1977), i.e.,

$$D_b = \frac{\phi(U - U_{mf})^{0.4}\,(H + 4.0\sqrt{A_0})^{0.8}}{g^{0.2}} \qquad (14)$$

In the present work, ϕ was experimentally determined by assuming that the bubble diameter, D_b, was equal to the column diameter

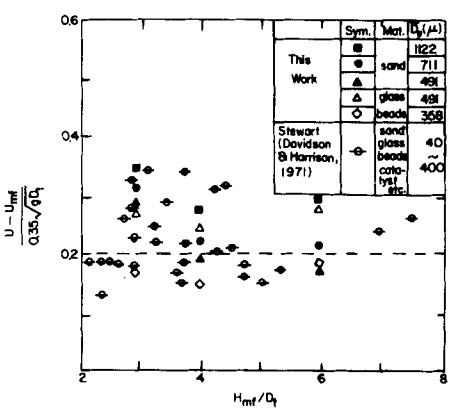

Figure 7. Experimental data on the onset of slugging.

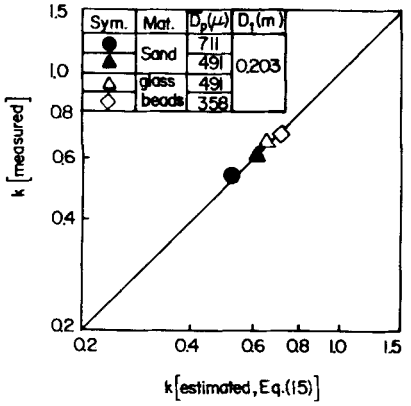

Figure 8. Plot of the measured k values against the estimated values.

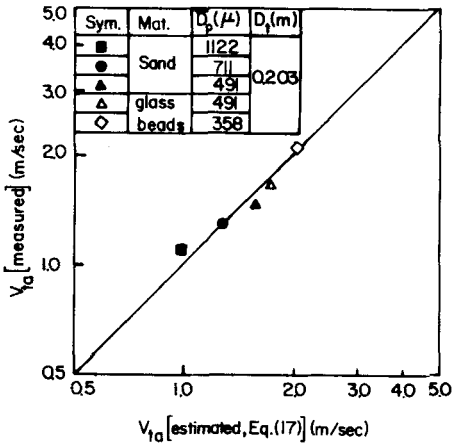

Figure 10. Plot of the measured V_{ta} values against the estimated values.

when the rise velocity of slugs was minimum. For example, D_b = 0.203 m at U/U_{mf} = 1.53 for the fluidized bed of sand with $\bar{D}_p$ = 0.000711 m (Figure 5). It appears that Model I and the available models described the results equally well. This is true also for other sets of experimental results. This suggests that the use of the one parameter equation, i.e., Eqs. 3 and 4, is satisfactory in estimating the rise velocity of bubbles or slugs.

The applicability of the two-phase theory in fluidized beds has been a controversial subject (e.g., Cranfield and Geldart, 1974; Xavier et al., 1978). However, a reasonably satisfactory description of the present results by Eq. 3 suggests that the two-phase theory may be applicable to our work. Since measurements of the bubble rise velocity in this work were conducted near the slug flow condition, it appears that the two-phase theory is at least applicable under such a condition; a comment to the same effect has been made by Grace (1981).

An attempt was made to correlate the values of k in Eq. 3 in bubbling bed regime and those of k' in Eq. 4 in the slugging bed regime for different fluidizing particles and column diameters. For air-sand and air-glass beads systems, we have obtained

$$k = 0.18\left(\frac{\bar{D}_p}{D_t}\right)^{-0.32}\left(\frac{\rho_s}{1000\rho_f}\right)^{-0.92} \tag{15}$$

in the bubbling bed regime, and

$$k' = 2.43\left(\frac{\bar{D}_p}{D_t}\right)^{-0.5}\left(\frac{\rho_s}{1000\rho_f}\right)^{-4.2} \tag{16}$$

in the slugging bed regime. Note that Eq. 15 is based on the data obtained using the beds with D_t = 0.203 m and on the bubble parameters estimated from Eq. 14. The experimental values of k and k' are well correlated according to these expressions, as can be seen in Figures 8 and 9, respectively. It can be observed that the k values range from 0.53 to 0.70, and the k' values from 1.03 to 3.80. These values are in good agreement with the results obtained by the previous investigators (e.g., Davidson and Harrison, 1963; Ormiston et al., 1965). For the rise velocity of a pressure wave in the turbulent bed regime (0.203 m diameter beds), Model I assumes that it is constant and can be expressed by Eq. 10, i.e.,

$$V_t \simeq V_{ta} \tag{10}$$

An empirical expression has been obtained for estimating the values of V_{ta} for the air-sand and air-glass beads beds with D_t = 0.203 m, i.e.,

$$V_{ta} = 0.134\left(\frac{\bar{D}_p}{D_t}\right)^{-0.56}\left(\frac{\rho_s}{1000\rho_f}\right)^{-1.16} \tag{17}$$

This correlation is compared with the experimental values of V_{ta} in Figure 10. As indicated by the figure, the agreement is good.

It should be noted that all three correlations, i.e., Eq. 15, 16 and 17 given in the above paragraph, indicate that bubbles, slugs or pressure waves rise faster in fluidized beds with smaller particle density and smaller relative size between the particle and the column, i.e., $\bar{D}_p/D_t$, for the same value of $(U - U_{mf})$. This trend is in agreement with the observations made by Rowe and Partridge (1965) and Littman and Homolka (1970).

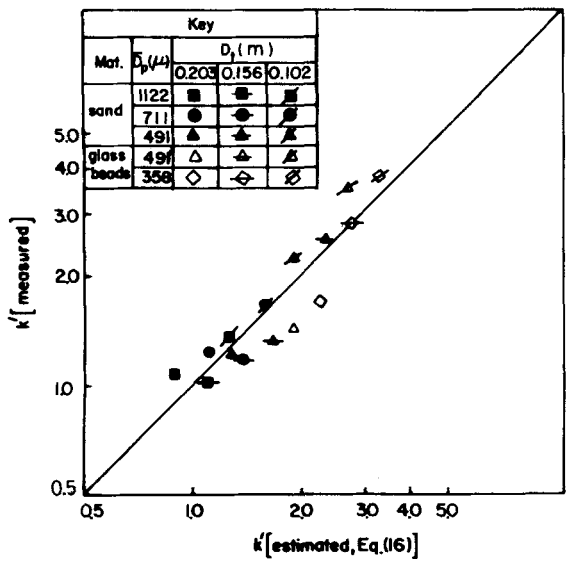

Figure 9. Plot of the measured k' values against the estimated values.

Model II

Model II has also been fitted to the experimentally determined rise velocities of bubbles, slugs, and pressure waves. The resultant equations are:

$$\left[\frac{V_b - V_{bmi}}{V_{bma} - V_{bmi}}\right] = \left[\frac{U - U_{mf}}{U_{ms} - U_{mf}}\right]^{0.44(1000\bar{D}_p/D_t)^{-1.3}(\rho_s/1000\rho_f)^{-0.9}} \tag{18}$$

$$\left[\frac{V_s - V_{smi}}{V_{sma} - V_{smi}}\right] = \left[\frac{U - U_{ms}}{U_{mt} - U_{ms}}\right]^{1} \tag{19}$$

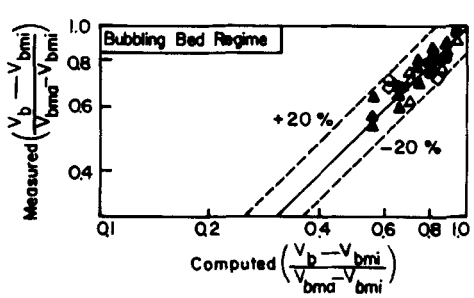

Figure 11(a). Comparison between the measured dimensionless bubble rise velocity and that computed from Equation (18). (See Fig. 9 for symbols)

TABLE 2. RISE VELOCITIES OF BUBBLES OR SLUGS MEASURED AT DIFFERENT SEPARATION DISTANCES OF PRESSURE TAPS ($\overline{D}_t$ = 0.203 m)

Material	$\overline{D}_p$(m)	Tap Position (m above the Distributors)	Separation Distance (m)	Avg. Rise Velocity of Bubbles or Slugs (m/s)			
				$\frac{U}{U_{mf}} = 1.25$	$\frac{U}{U_{mf}} = 1.5$	$\frac{U}{U_{mf}} = 1.75$	$\frac{U}{U_{mf}} = 2.0$
Sand	0.000711	0.40–0.59	0.19	0.73	0.82	0.95	1.16
		0.45–0.59	0.14	0.75	0.84	0.96	1.19
		0.49–0.59	0.10	0.78	0.98	1.02	1.47
Sand	0.000491	0.40–0.59	0.19	0.75	1.00	1.15	1.29
		0.45–0.59	0.14	0.81	1.01	1.17	1.52
		0.49–0.59	0.10	0.81	1.06	1.28	1.63
Glass Beads	0.000491	0.40–0.59	0.19	0.70	1.09	1.30	1.52
		0.45–0.59	0.14	0.73	1.10	1.44	1.69
		0.49–0.59	0.10	0.74	1.10	1.61	1.95

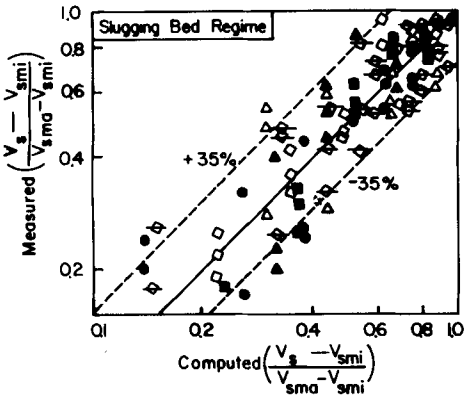

Figure 11(b). Comparison between the measured dimensionless slug rise velocity and that computed from Equation (19). (See Fig. 9 for symbols)

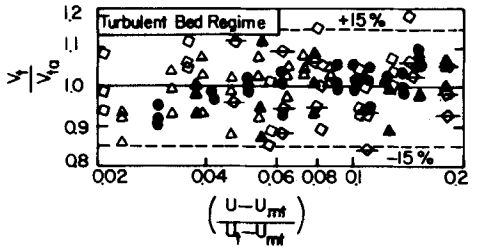

Figure 11(c). Plot of the measured (V_t/V_{ta}) against the term [($U - U_{mt}$)/($U_t - U_{mt}$)] of Equation (20). (See Fig. 9 for symbols)

$$\left(\frac{V_t}{V_{ta}}\right) = \left[\frac{U - U_{mt}}{U_t - U_{mt}}\right]^0 = 1 \tag{20}$$

The experimentally obtained values of $[(V_b - V_{bmi})/(V_{bma} - V_{bmi})]$ are compared with those computed from Eq. 18 in Figure 11(a), and the experimentally obtained values of $[(V_s - V_{smi})/(V_{sma} - V_{smi})]$ are compared with those computed from Eq. 19 and Figure 11(b); the experimentally obtained values of (V_t/V_{ta}) are plotted against the values of $[(U - U_{mt})/(U_t - U_{mt})]$ in Figure 11(c). It can be seen that the model describes the experimental results reasonably well. Note that, in fitting the above correlations to the data, the value of V_{bmi} was set equal to zero; the values of V_{smi}, V_{sma}, V_{ta}, U_{mf}, U_{ms} and U_{mt} were experimentally determined; and the value of U_t was estimated from Figure 9 in Chapter 3 of the monograph by Kunii and Levenspiel (1969).

To apply Model II for estimation of the rise velocities of bubbles, slugs, or pressure waves, the values of the parameters in the correlation equations, i.e., V_{bma}, V_{smi}, V_{sma}, V_{ta}, U_{mf}, U_{ms}, U_{mt} and U_t, need to be determined or estimated a priori. These values, except the values for U_{mf} and U_t which are available in the literature, can be roughly estimated by the following correlations based on the data obtained in this work.

$$V_{bma} \simeq \left(0.85 \frac{\rho_{\text{sand}}}{\rho_s}\right)(gD_t)^{1/2} - U_{mf} \tag{21}$$

$$V_{smi} \simeq \left(0.8 \frac{\rho_{\text{sand}}}{\rho_s}\right)(gD_t)^{1/2} - U_{mf} \tag{22}$$

$$V_{sma} \simeq V_{ta} \simeq \left(1.25 \frac{\rho_{\text{sand}}}{\rho_s}\right)(gD_t)^{1/2} - U_{mf} \tag{23}$$

$$U_{ms} \simeq 0.07\,(gD_t)^{1/2} + U_{mf} \tag{24}$$

$$U_{mt} \simeq 0.30\,(gD_t)^{1/2} + U_{mf} \tag{25}$$

It has been pointed out (Fan et al., 1981) that major fluctuations in the lower portion of a fluidized bed are caused by the formation of large bubbles in the upper portion of the bed, and thus pressure fluctuation signals detected in the lower portion of the bed coincide with each other in the major fluctuations. This prevents the application of the technique in the lower portion of the bed. The technique, however, can be used for any pair of locations in the upper portion of the bed, where the motion of bubbles causes pressure fluctuations.

It should be noted that the separation distance between two taps has some effects on the result. Table 2 shows that the measured bubble rise velocity tends to be greater when the separation distances are shorter; however, the deviation is not large except when the distance is excessively short. According to Oki et al. (1977), the correlation between the two measured signals becomes smaller as the distance increases, and thus, it becomes difficult to locate the peak of the cross-correlation function. Conversely, if the distance becomes small, the directional characteristics become less distinct and the error caused by digitizing the signal to compute the transit time becomes large. It appears that a distance approximately equal to or larger than the diameter of the column is a suitable choice.

ACKNOWLEDGMENT

The authors are grateful to the Department of Energy for financial support of this work under Contract DE-AC21-81MC16310.

NOTATION

A_0 = catchment area for a bubble stream at the distributor plate
D_b = equivalent bubble diameter
$\overline{D}_p$ = average particle diameter
D_t = bed diameter
g = gravitational acceleration
H = height in the bed
H_{mf} = height in the bed at the minimum fluidization condition

k = coefficient, defined in Eqs. 1 and 3
k_1, k_2 = coefficient, defined in Eq. 8
k' = coefficient, defined in Eq. 4
k_1', k_2' = coefficient, defined in Eq. 9
L = distance between taps
t = time
T = time period
U = superficial gas velocity
U_b = rise velocity of an isolated bubble
U_{mf} = superficial gas velocity at the minimum fluidization condition
U_{ms} = superficial gas velocity at the minimum slug condition
U_{mt} = superficial gas velocity at the minimum turbulent condition
U_s = rise velocity of an isolated slug
U_t = terminal particle velocity
V_b = bubble rise velocity in the bubbling bed regime
V_{bma} = maximum bubble rise velocity in the bubbling bed regime
V_{bmi} = minimum bubble rise velocity in the bubbling bed regime, zero
V_f = velocity of a fluctuation waveform
V_s = slug rise velocity in the slugging fluidized bed regime
V_{sma} = maximum slug rise velocity in the slugging bed regime
V_{smi} = minimum slug rise velocity in the slugging bed regime
V_t = rise velocity of pressure wave in the turbulent bed regime
V_{ta} = average rise velocity of pressure wave in the turbulent bed regime
$X(t)$- = random variables
$Y(t)$ = random variable

Greek Letters

α, β, γ = constants, Eq. 11
α' = constant, Eq. 12
τ = shifted time
τ_m = transit time where the cross-correlation function is maximum
ϕ = coefficient defined in Eq. 14
ϕ_{xy} = cross-correlation function between $X(t)$ and $Y(t)$
ρ_f = density of fluid
ρ_s = density of fluidizing particles
ρ_{sand} = density of sand

LITERATURE CITED

Cranfield, R. R., and D. Geldart, "Large Particle Fluidization," *Chem. Eng. Sci.*, **29,** 935 (1974).

Darton, R. C., R. D. Lanauze, J. F. Davidson, and D. Harrison, "Bubble Growth Due to Coalescence in Fluidized Beds," *Trans. Int. Chem. Eng.*, **55,** 274 (1977).

Davidson, J. F., and D. Harrison, *Fluidized Particles*, Cambridge University Press, New York, NY (1963).

Davidson, J. F., and D. Harrison, *Fluidization*, Academic Press, Inc., New York, NY (1971).

Davidson, J. F., R. C. Paul, J. S. Smith, and H. A. Duxbury, "The Rise of Bubbles in a Fluidized Bed," *Trans. Inst. Chem. Engrs.*, **37,** 323 (1959).

Fan, L. T., Tho-ching Ho, S. Hiraoka, and W. P. Walawender, "Pressure Fluctuations in a Fluidized Bed," *AIChE J.*, **27,** 388 (1981).

Godard, K., and J. F. Richardson, "Bubble Velocities and Bed Expansions in Freely Bubbling Fluidized Beds," *Chem. Eng. Sci.*, **24,** 663 (1969).

Grace, J. R., "Fluidized Bed Reactor Modeling: An Overview," *ACS Symp. Ser.* No. 168, p. 3, American Chemical Society, Washington, DC (1981).

Harrison, D., and L. S. Leung, "Bubble Formation at an Orifice in a Fluidized Bed," *Trans. Inst. Chem. Engrs.*, **39,** 409 (1961).

Kang, W. K., J. P. Sutherland and G. L. Osberg, "Pressure Fluctuations in a Fluidized Bed with and without Screen Cylindrical Packings," *I&EC Fund.*, **6,** 449 (1967).

Kunii, D., and O. Levenspiel, *Fluidization Engineering*, John Wiley and Sons, Inc., New York (1969).

Lanneau, K. P., "Gas-Solids Contacting in Fluidized Beds," *Trans. Inst. Chem. Engrs.*, **38,** 125 (1960).

Lee, Y. W., *Statistical Theory of Communication*, John Wiley and Sons, Inc., New York, NY (1960).

Littman, H., and G. A. J. Homolka, "Bubble Rise Velocities in Two-Dimensional Gas-Fluidized Beds from Pressure Measurements," *Chem. Eng. Prog. Sym. Ser.*, **66,** (105), 37 (1970).

Matsen, J. M., S. Hovmand, and J. F. Davidson, "Expansion of Fluidized Beds in Slug Flow," *Chem. Eng. Sci.*, **24,** 1743 (1969).

Oki, K., W. P. Walawender, and L. T. Fan, "The Measurement of Local Velocity of Solid Particles," *Powder Technology*, **18,** 171 (1977).

Oki, K., W. P. Walawender, and L. T. Fan, "An Inexpensive and Simple Correlator for Velocity Measurement," *I&EC Fund.*, **17,** 358 (1978).

Ormiston, R. N., F. R. G. Mitchell, and J. R. Davidson, "The Velocities of Slugs in Fluidized Beds," *Trans. Inst. Chem. Engrs.*, **43,** 209 (1965).

Park, W. H., W. K. Kang, C. E. Capes, and G. L. Osberg, "The Properties of Bubbles in Fluidized Bed of Conducting Particles as Measured by an Electroresistivity Probe," *Chem. Eng. Sci.*, **24,** 851 (1969).

Pyle, D. L., and D. Harrison, "The Rising Velocity of Bubbles in Two-Dimensional Fluidized Beds," *Chem. Eng. Sci.*, **22,** 531 (1967a).

Pyle, D. L., and D. Harrison, "An Experimental Investigation of the Two-Phase Theory of Fluidization," *Chem. Eng. Sci.*, **22,** 1199 (1967b).

Reuter, H., "Mechanismus der Blasen im Gas-Feststoff-Fleissbett," *Chemie-Ingenieur-Technik*, **35,** 98, 219 (1963).

Rigby, G. R., G. P. Van Blockland, W. H. Park, and C. E. Capes, "Properties of Bubbles in Three Phase Fluidized Beds as Measured by an Electroresistivity Probe," *Chem. Eng. Sci.*, **25,** 1729 (1970).

Rowe, P. N., and B. A. Partridge, "An X-Ray Study of Bubbles in Fluidized Beds," *Trans. Inst. Chem. Engrs.*, **43,** 157 (1965).

Swinehart, F. M., "A Statistical Study of Local Wall Pressure Fluctuations in Gas Fluidized Column," Ph.D. Dissertation, University of Michigan (1966).

Toei, R., R. Matsuno, H. Kojima, Y. Nagai, K. Nokagawa, and S. Yu, "Behavior of Bubbles in Gas-Solid Fluidized Beds," *Kagaku Kogaku*, **29,** 851 (1965).

Werther, J., and O. Molerus, "The Local Structure of Gas Fluidized Beds—II. The Spatial Distribution of Bubbles," *Int. J. Multiphase Flow*, **1,** 123 (1973).

Xavier, A. M., D. A. Lewis and J. F. Davidson, "The Expansion of Bubbling Fluidized Beds," *Trans. Inst. Chem. Engrs.*, **56,** 274 (1978).

Manuscript received May 12, 1981; revision received January 14, and accepted January 28, 1982.